Quick Radar / Optical Super Observation for Deep Space

Josh Minneti, Andrew Laffely, Nathan Stallworth
Rich Ghrist, Edward Fernandez, Justin Wilmes
MITRE Corporation

Abstract

Traditionally the Space Domain Awareness (SDA) architecture uses a hand-full of "exquisite" sensors to collect information on deep space objects. Radar systems provide excellent range and good range rate at Geosynchronous Earth Orbit (GEO) distances, but, due to the radar beam width at those ranges, absolute positional errors in the tens of kilometers degrade the overall accuracy of the observation data. Conversely, optical systems produce highly accurate angle measurements but lack range data, thus requiring long tracks to adequately determine orbits. In either case, using radar and optical observation data independently can cause slow or inaccurate orbit determinations for deep space objects. With the advent of inexpensive optical devices, it is practical to dedicate one such system to existing radar systems. Using the same mission planner to task both devices in tandem, and combining the data (near) real-time, reduces the absolute positional error of radar/optical joint "super" observations to fractions of the radar system's alone. This paper outlines the algorithm developed to fuse radar and optical data in real-time for geographically separated radar and optical assets. Additionally, experimental and simulated results illustrate the reduction in observational error when radar and optical data are combined in real-time. Finally, this paper demonstrates the resulting improvement in space domain awareness when leveraging this more accurate observational data.

1. INTRODUCTION

It is well understood that radar and optical systems provide complementary measurements on space objects.[1] Fig. 1 highlights these differences. Radars provide highly accurate range information but suffer potentially large errors in angles, especially when observing deep space objects. This creates a plate or pancake-shaped positional measurement uncertainty. Optical systems provide excellent angle information but cannot instantaneously predict range, resulting in a straw-like uncertainty. Using the best attributes from each system concurrently greatly reduces the position measurement errors.

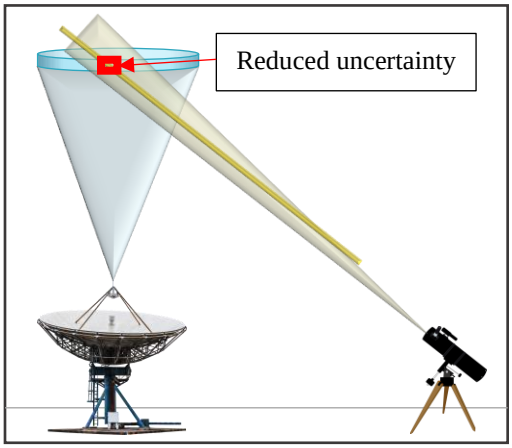

Fig. 1. Complementary Position Measurements for Different Sensor Types

The current approach is to use these systems independently, taking all possible observations over a long time, potentially a full day, to create an orbit model from geographically dispersed sensors. This paper proposes a different, potentially more efficient, approach. Given the improvement and cost reduction of small-aperture telescope systems, it is possible to directly pair inexpensive optical systems with existing radar systems, either at the same physical location or dispersed for optimal viewing conditions. This pairing could record highly accurate data at night on space objects, resulting in higher-quality orbits with reduced required viewing time. Given recent and

ongoing improvements to daylight optical tracking, it may be possible to utilize this combined sensor for a larger portion of each day.[2] The approach here does not result in improved daily orbits over the independent system method being used today. It does have the potential to make radar systems, costing millions to operate annually, more efficient by adding a $50k optical co-system.

This paper first outlines an algorithm to combine the observations (obs) from radar and optical systems. This is a starting point for evaluating the application of the resulting "super-ob". Second, it demonstrates the operation of the algorithm on real-world collection data from an inexpensive optical system and an Ultra High Frequency (UHF) radar. This data is compared to high precision "truth" ephemeris data to quantify the error of the combined observations against that of the radar-only observations. Next, these error characterizations inform larger scale simulations to probabilistically determine how long the new super-ob methodology takes to perform accurate Orbit Determination (OD) vs. a radar-only approach. Ultimately, the results lead to the assertion that combining radar and optical data in real-time yield dramatically more accurate observational data, resulting in greatly reduced time to achieve an accurate OD. Finally, the paper presents a hypothetical study showing the improved throughput of a radar system employing an optical co-system.

2. COMBINING OBSERVATIONS

"Observations," in this context, refer to topocentric feature data generated as a final output of a radar or optical system. In the case of a radar, Range, Azimuth, Elevation (RAE) and Range Rate are provided. Alternatively, an optical system yields Right Ascension, Declination, (RA-Dec). The first task is to determine a methodology that combines the positional radar and optical data from geographically dispersed sites. A simple trigonometric approach to solve this problem is shown in Fig. 2, below:

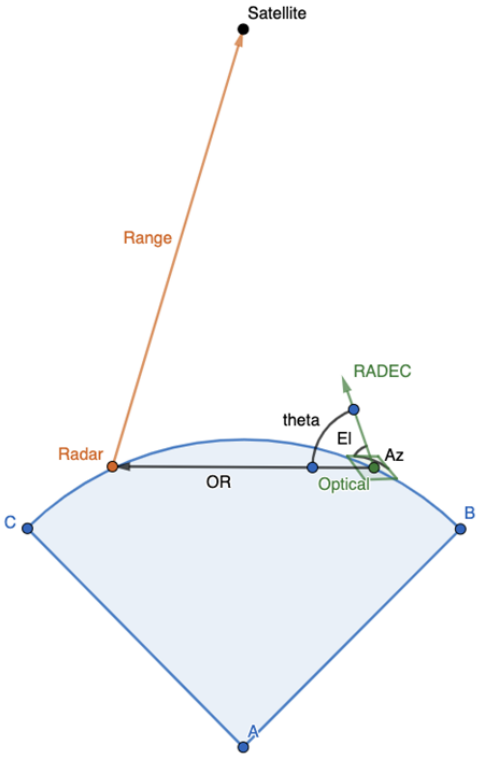

Fig. 2. Trigonometric Approach to Combining Radar and Optical Observation Data

The blue arc (***ABC***) grossly represents the surface of the Earth, simply to indicate the radar site and optical sites are geographically dispersed. Additionally, please note the ***Range*** quantity from the radar is not considered a vector in this analysis. The radar angle data are ignored due to their inherent error. To merge the observation data, solve the Side-Side-Angle (SSA) triangle generated by determining the ***OR*** vector and angle ***θ (theta)***. The plane generated by

the RA-Dec data (converted to Azimuth and Elevation [Az-El]) from the optical and the ***OR*** vector appropriately align the radar range scalar, allowing to solve for the range with respect to the optical position. Thus, RAE data are generated with respect to the optical using the optical angles, the radar range, and the geographic locations of the sensor sites. A more specific description of the algorithm follows:

The "Combination Algorithm" expects the following inputs:

- Radar Geographic Location (Latitude, Longitude, and Elevation)
- Optical Geographic Location (Latitude, Longitude, and Elevation)
- Observation Data
    - Timestamp (observations must be close in time to be combined)
    - Optical RA-Dec
    - Radar Range

Given the appropriate inputs, the following steps are executed:

1. Convert the optical RA-Dec to Az-El
2. Calculate ***OR*** using the site locations, convert to topocentric frame with respect to the optical
    a. Convert the site locations to the Earth-centered-inertial (ECI) frame specified by the true equator and mean equinox (TEME)
    b. Calculate the ECI TEME vector from the optical to the radar
    c. Convert the ECI TEME vector to the same topocentric frame as the optical Az-El
3. Determine $\boldsymbol{\theta}$, the angle between the optical Az-El and ***OR*** vector
4. Solve the Side-Side-Angle (SSA) triangle generated by radar range, ***OR***, and $\boldsymbol{\theta}$ to solve for the optical range scalar
5. Return RAE data with respect to the optical site

The steps presented above are readily accomplished with any modern Astrodynamics software package, and this simplicity is what made the algorithm attractive. There are a couple of assumptions and limitations that must be considered. First, and potentially most obvious, the radar and optical data must be aligned in time for the most accurate results. The motion of the space object relative to the sensor sites will dictate how well time-aligned the observation data must be. Second, solving an SSA triangle can result in an ambiguous case where 2 triangles meet the specifications. Specific orbital physics reality checks can filter this ambiguous case based on the reported angle from the radar and known attributes of the space object.

After implementing the Combination Algorithm, it was tested with simulated data. Ephemeris for 22 known space objects in GEO and Medium Earth Orbit (MEO) were used to create 719 simulated observation data points for simulated radar and optical systems. The appropriate look-angles were used to represent radar and optical sites separated by hundreds of miles. The observations were separately noised according to accuracy parameters for an Ultra High Frequency (UHF) radar and a 12-inch Ritchey-Chretien Telescope system. Finally, the noised observation data were combined using the Combination Algorithm described above to form a set of super-obs. Analyzing this set confirmed that the components of each observation correctly mirrored the accuracies of the better sensor, i.e. the range accuracy of each super-ob was driven by the accuracy of the range in the radar model, and the angular accuracies followed that of the optical system model. It should be noted that the angular accuracy standard deviation for the radar system was set to two orders of magnitude wider than the optical angle standard deviation. In addition to accurately representing the angular performance differences, this also made it easy to show the super-ob was truly pulling the parameters from the correct sensor. In the combined observations, an increase in the range bias and sigma was seen, which was attributed to numerical coordinate transformation errors and mismatches. As the absolute values of these were very small in comparison to the angle errors (<1% of the total position error from the radar at GEO ranges), no attempts were made to optimize the algorithm further.

The results of this comparison are shown in Table *1*. The range statistics of the super-obs are comparable to those of the radar-only observations, though both the bias and sigma values increase (34% and 43%) after combination. The angle error statistics of the super-ob were consistent with the angle errors collected for the optical system. Elevation bias was off by 20% but the sigma values for both Azimuth and Elevation had only 3% deviation from the optical alone statistics. This confirms that the tool produces super-obs with the best statistical error bounds from the radar and optical systems.

Parameter	Mean Error Ratio (Bias Ratio)	Standard Deviation of Error Ratio (Sigma Ratio)
Range super-ob/radar ob	1.34	1.43
Azimuth super-ob/optical ob	0.936	1.03
Elevation super-ob/optical ob	1.20	0.970

Table 1. Combination Algorithm Results

3. REAL DATA COLLECTION

With confidence that the Combination Algorithm works in simulation, a real-world test was conducted to serve two purposes: first, to generate observations that further verify the Combination Algorithm and second, to perform a limited characterization of the observations to better inform the radar and optical models. Both goals required comparing real-world results with truth data to measure the error of the observations. To that end, collections focused on satellites that either broadcast their GPS location or those tracked by the International Laser Ranging Service (ILRS). These objects have the most accurate publicly available ephemeris data.

For the collection itself, the US Air Force tasked the UHF radar at Eglin AFB. The optical was a portable system consisting of a Software Bisque Paramount ME I mount, a Guan Sheng Optical (GSO) Ritchey-Chretien Telescope, an Andor Zyla 4.2 sCMOS camera, and other various control hardware, set up in Colorado Springs CO. Tasks were aligned by a pre-defined schedule.

4. REAL DATA RESULTS

Overall, the results are very positive, but limited in scope due to timing constraints and cloud cover at the optical site. The best data was from a GEO object, ANIK F1-R, on March 11, 2020. 150 Flexible Image Transport System (FITS) images were collected between 0321-0336 Coordinated Universal Time (UTC), which yielded 97 observations from the optical site. Shortly thereafter, clouds rolled in and remained throughout the night. During the same time span, the UHF Radar generated 24 observations and continued to collect a total of 138 observations for ANIK F1-R. To begin the analysis, the radar data was compared against ephemeris truth. Fig. 3 serves to illustrate the comparison of *all* the radar observations against truth, plotting the measured errors in range, azimuth, elevation, and position. In each plot, zero error is highlighted on the y-axis.

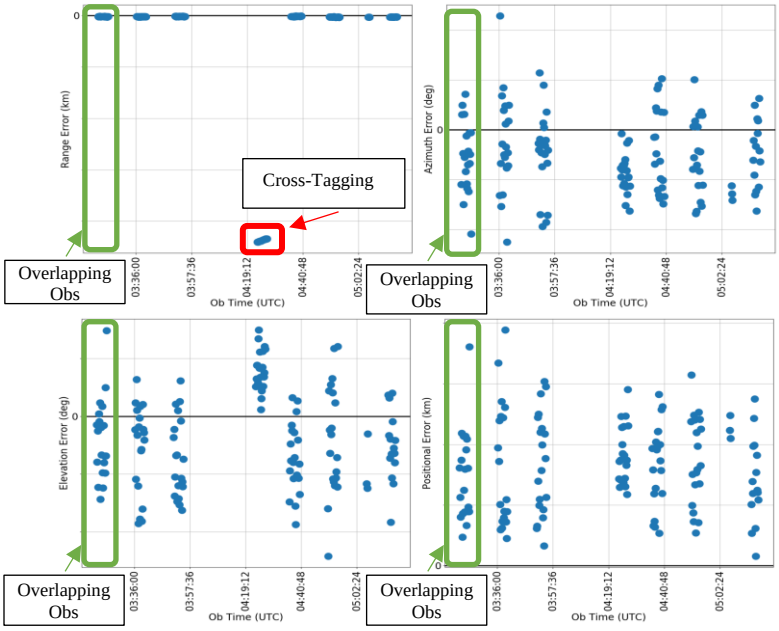

Fig. 3. Radar Observations vs Truth

Additionally, a specific track taken near 0419 UTC appears to be incorrectly correlated (cross-tagged) to ANIK F1-R. This track was dropped for the analysis. Next, the green areas highlight the timeline are the ones that overlap with the optical obs. This area contains the radar data that was passed to the Combination Algorithm. The takeaway from Fig. 3 should be that after removing the cross-tag data, the radar data that overlaps the optical data statistically represents the radar performance on this object. Therefore, it gave an ability to spot check the Combination Algorithm using the real data. In addition, the full radar data set was used to verify the model of UHF radar error parameters.

Fig. 4 shows the results of applying the Combination Algorithm to the overlapping observations from Fig. 3. The candidates for combination were limited to only those observations that were within 3 seconds of each other. This further reduced our usable data to only 12 of the original 24 radar observations. This identifies a key constraint in the system set up. To successfully meet the efficiency application presented later in this paper, the timing of the radar and optical observations would have to be more tightly coordinated. This experiment was limited to phone coordination and pre-planned data collection. To improve effectiveness the optical system would need to be directly tied to the radar mission planning system. Doing this would ensure all observations align in time. Even with the limited dataset, orbit determination from the super obs was successful. This closed the loop for the evaluation. The key point from Fig. 4 shows that the angle sigma (standard deviation) of the combined observations are clearly much lower than the radar-only data.

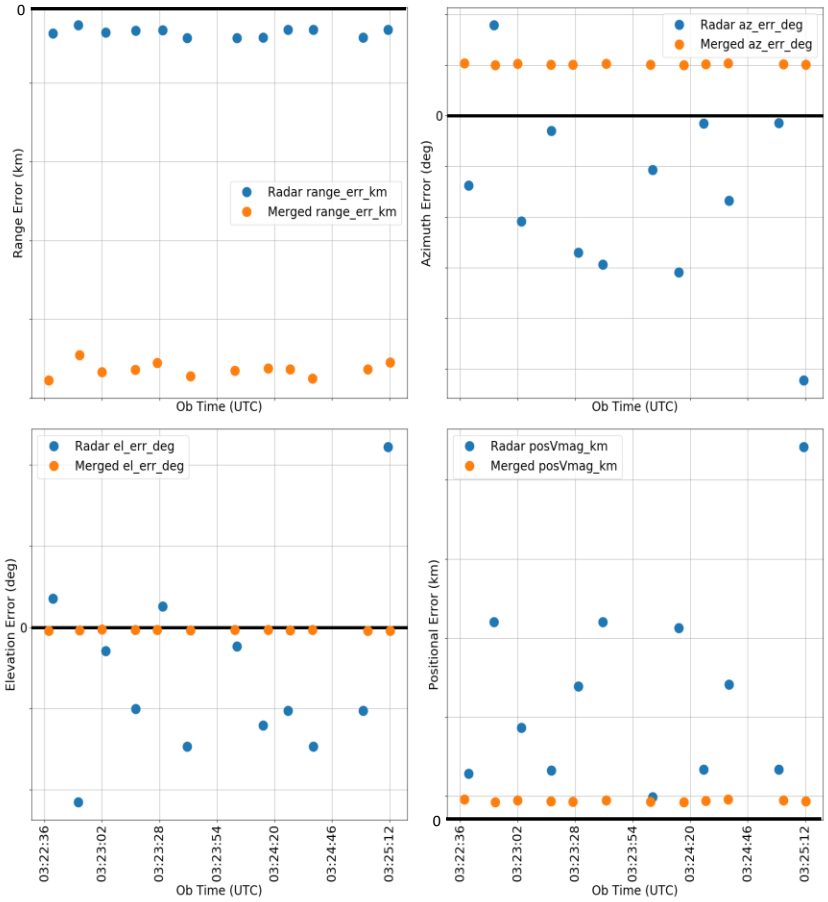

Fig. 4. Radar Errors vs Combined Errors

This is also summarized in Table 2. Despite the time differences, the average positional error for the combined observations, now super-obs, were reduced by nearly 1/3 over the radar-only observations. More impressively and importantly, the sigma of the positional error is reduced by 99%. The bulk of these corrections came from much tighter angle standard deviations from the optical system. The range average or bias error in the combined

observations increased by a factor of nearly 12 over the radar system. This highlights the potential rounding errors in the Combination Algorithm discussed earlier in the paper. Bias errors can be measured and calibrated out in operational systems. The range standard deviation for the super-ob was on par with the original radar-only data. While the data sample size was small, it is consistent with the much larger modeling sample to conceptually spot check the toolset and approach.

Parameter	Average (Bias)	Standard Deviation (Sigma)
Range	Up by factor of 12	Up marginally
Azimuth	Down marginally	Down by factor of 130
Elevation	Down by factor 17	Down by factor of 200
Position	Down by factor of 2.5	Down by factor of 100

Table 2. Parameter Errors of Super-Obs Relative to Radar Obs

5. METHODOLOGY TO DETERMINE SYSTEM EFFECTIVENESS

With confidence in combining observation information, the next step was to show that the improved combined sensor performance would indeed make positive impact on the overall mission and efficiency in radar operations. The hypothesis is that combining observations in real time allows the radar system to more quickly complete each task and thus would allow higher throughput for the sensor. In the model environment, clean observations were generated from a Two Line Element Set (TLE) within the following time-frame: March 11, 2020 0000-2359 UTC at 20 second intervals, yielding 4,319 observations. These would be considered truth observations, meaning no error is introduced. All were representative of the GEO object, ANIK F1-R, collected in the real data experiment. Other orbit regimes were not evaluated. Each perfect observation was noised 100 times based on the performance statistics of the radar and combined systems. This process was independently repeated to create 100 noised sets of the 4319 original observations for both the radar and the combined system. Orbits were developed using the sets of noised observations, performing orbit determinations using observations in subsets of 3, 6, 9, …90 obs to provide thousands of derived orbits in TLEs. Note: stepping the obs by 3 was based on performing orbit determination every minute. Other stepping values could have been used. Each of the resulting TLEs was then propagated for 30, 60, 90 and 120 minutes in the future, and the resulting position was compared to the original (truth) TLE propagated for each object. This created an absolute position error data point for each generated TLE against the truth TLE. The position errors were organized by the number of observations used to create the TLEs and then statistically analyzed for performance of the radar-only observations versus the super-obs. The next section highlights some of the results that were characteristic of the large data sets.

6. SELECTED RESULTS

To demonstrate the potential of the super-ob, a notional mission success criteria is proposed. This section only addresses a couple of permutations of the mission success criteria. The mission and sensor owners would have to identify true success critiria. The approach to attain this data could be adapted to their critirea.

Fig. 5 is representative of a typical output for the success criteria used in this study. Accuracy of the generated and propagated orbit is used as the measure for mission success. That is, for the sensor, either radar or combined, how well do the observations collected produce an orbit accurate enough to correctly predict the future position of the object? Fig. 5 shows a success threshold of 50km Root Sum Squared (RSS) position error after propagating the generated orbit 90 minutes from the last observation. The y-axis shows the percentage of orbits generated from obervations that meet the 90 minute/50km accuracy criteria. The x-axis shows the radar task time on the object. Recall, the modeled system produces a single observation every 20 seconds. During real operations, this value would depend on the specific radar, optical system and object. Twenty seconds represents a best guess at average performance but could be adjusted and does not change the relative results. With this, orbits represented by TLEs, are generated every minute for both the radar and combined sensor. The first data point shows orbits that are derived based only on three observations. The second data point uses 6 observations, the third uses 9 observations, etc. The orange line (left/top in the graph) shows the results for the super-obs of the combined sensor. The blue line (right/lower in the graph) shows the results for radar-only observations.

Fig. 5 shows the combined sensor produces orbits meeting the success criteria 90% of the time after only 4 minutes in track, i.e. using 12 super-obs. The radar model takes 28 minutes (84 observations) to produce similar results. That is a factor of 7 times more efficient per task. Note: Fig. 5 was completed on a set of data different than explained in Section 5. It was completed before obtaining real-world statistics on sensor performance. Note that the trend between this data and the constrained data of Fig. 6 is consistent.

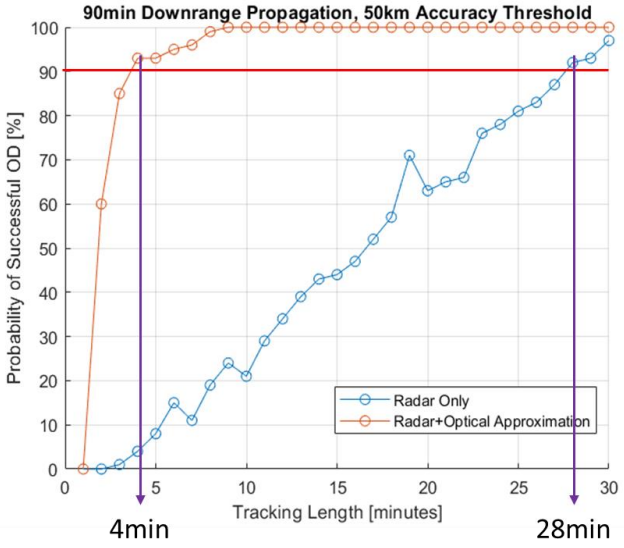

Fig. 5. Mission Success, Super-Ob vs. Radar-Only

Fig. 6 shows a subset of the modeled data as described in Section 5. For this graph, the simulation is constrained to only use the scenario and error statistics found in the real-world data collect. The trend is the same as the model-only data confirming the overall modeling approach.

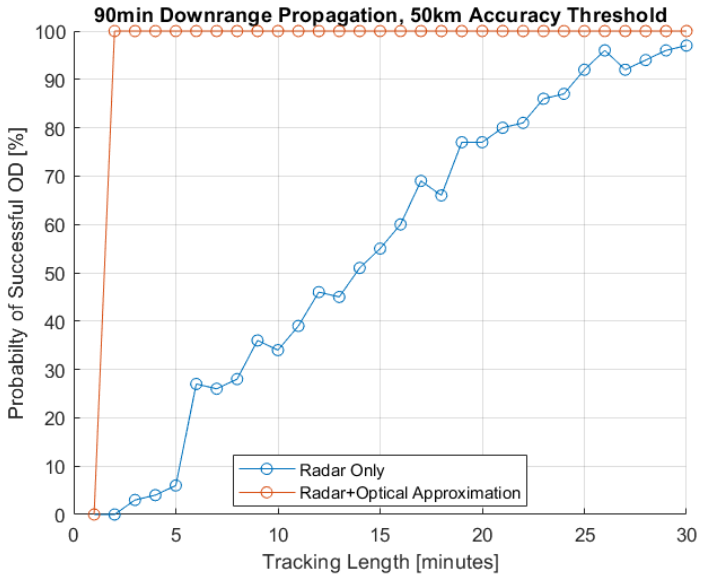

Fig. 6. Mission Success for Verified Model Scenerio, Super-Ob vs. Radar-Only

Finally, Fig. 7, shows a different permutation of the mission success critiria with the real world based data set. If the future error threshold is reduced from 50km to 20km the radar-only obs cannot meet the 90% effectiveness mark in

the alloted time. The radar alone cannot reach even 65% within 30 minutes, while the super-ob system reaches 100% within 3 minutes.

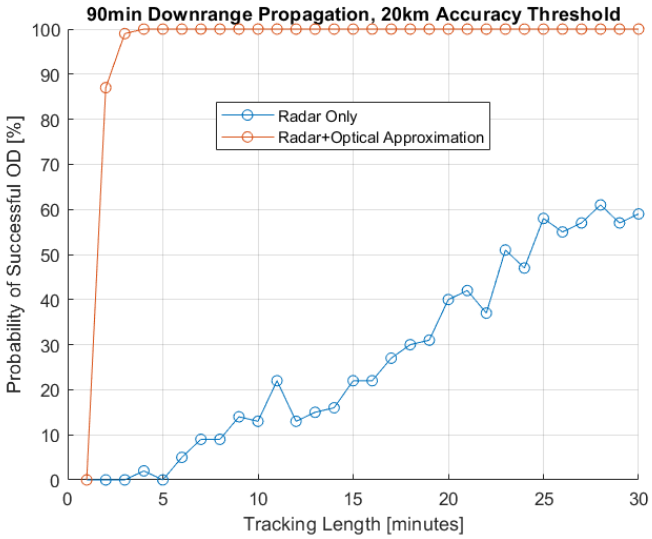

Fig. 7. More Challenging Mission Success for Verified Model Scenerio, Super-Ob vs. Radar-Only

These results clearly indicate utilizing the Combination Algorithm in real-time can yield more accurate observation data and that accuracy has a dramatic effect on mission success. That said, these results are not without some limitations. Recall the model parameters and simulation results are based on a very limited set of real-world collections, thus the generalizability of the noising parameters must be done with caution. For this paper, it is clearly reasonable to assert that for ANIK F1-R on March 11, 2020, the optical and radar systems used for this analysis generated super-obs with much higher fidelity than the radar alone. We showed in Comparing Fig. 5 vs. Fig. 6 that results are consistent for multiple objects, though additional research is required to generalize any findings across orbit regimes and object sensitivity (radar cross-section, reflectivity, etc). Despite these limitations, this work provides a powerful argument both for additional research to broaden the understanding of the accuracy of the Combination Algorithm and efforts to implement real-time coordination between radar and optical systems.

7. APPLICATION

This section attempts to quantify what the improved task time would do for overall radar system performance. A completed task is the collection of enough observations to meet the OD success criteria described in Section 6. It serves only as a sketch of one possible application of the results. From the models in this analysis, the radar-only system can successfully complete one GEO task in 28 minutes. For generality, a three-minute period is added to each task for setup or slewing. This is an approximation for a responsive dish system. Phased array systems would respond nearly instantaneously. This means that the generic radar system alone will be able to compete a task in a total of 31 minutes. For the radar-optical combined system, assuming the same 3-minute set up time between tasks, the time to complete is 7 minutes. The combined system will only function during night hours, averaging about 50% of the time. These two different throughput values are plotted for a full day, assuming clear skies in, Fig. 8.

To further illustrate the break down between radar-only and radar-optical performance, the two separate systems' tasking completion rates are shown in Table 3. During the daytime, without optical supplementation, roughly only two GEO objects could be tracked per hour to meet the desired OD accuracy. However, during the nighttime, due to the reduction in necessary tracking time achieved by the addition of the optical system, the throughput increased to roughly 9 satellites tracked per hour. Over a 24-hour collection period the radar-only system collects enough data to produce a total of 46.5 accurate orbits, whereas the radar-optical system produces accurate orbits on 126 objects.

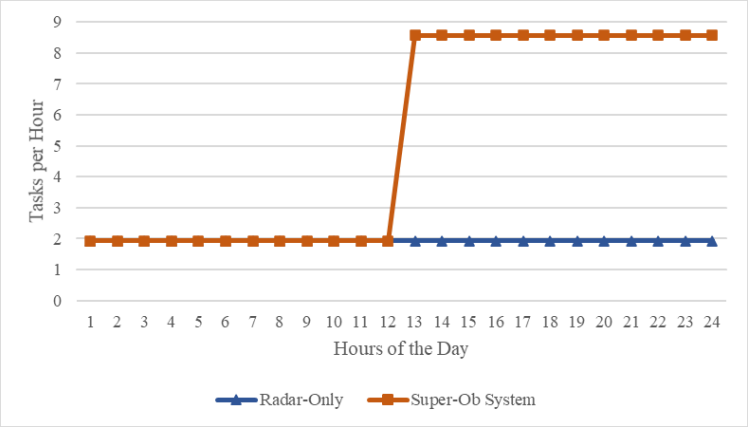

Fig. 8. Throughput of Radar-Only vs. Super-Ob System

Radar-Optical Super-Ob System:		**Radar-Only:**	
Avg Number of Tasks (per hr.) Daytime	1.9	Avg Number of Tasks (per hr.)	1.9
Avg Number of Tasks (per hr.) Nighttime	8.6	Total Number of Tasks (24 hr.)	**46.5**
Total Daytime Tasks (12 hr.)	23.3		
Total Nighttime Tasks (12 hr.)	102.8		
Total Number of Tasks (24 hr.)	**126.1**		

Table 3: Daily Throughput of Radar vs. Radar-Optical System

8. CONCLUSION

This paper presented a method to combine, in near real time, radar and optical observations to create a super-ob, taking advantage of the complementary uncertainties of the two sensor systems to produce highly accurate positional information. With real-world radar and optical systems, it showed that generation of these super-obs was possible using the basic tool developed in this study. It also used the real data as a "spot check" to drive much larger scale simulations to evaluate the benefits of using super-obs over radar-only obs. It showed cases where the super-ob reduced collect time by a factor of 7 when using the proposed mission success criterion of 50km RSS positional error 90 minutes after the completion of observations. With a more stringent threshold of 20km error, the radar-only solution does not converge within the allotted task time while the super-ob continues to perform well after the first few observations. Finally, it outlines an application for such a system. If the sensor system is tasked to provide quality data, meeting a success criterion like that proposed in this paper, then a notional combined system nearly triples the daily throughput when compared to the radar component alone.

Care must be taken in using the results. This paper attempts to illuminate the full approach from start through application, and thus provides a potential proof of concept. More work could be completed in each section above. For example, the radar model is assumed to be a very capable UHF system with large antenna area. Higher frequency (S, C, and X-Band) systems exist for SDA. With higher frequencies the angle error of the radar system could drop, thereby diminishing the benefit of adding an optical co-sensor. Still, the fact that purchasing and operating a $50,000 optical sensor is far less expensive than purchasing and operating the multi-million dollar SDA radar systems, there is little risk to adding optics to nearly all the SDA radars, even if the improvement is marginal. More effort, including real-world data collection, should be accomplished across other orbit regimes and conditions.

9. REFERENCES

[1] R Stottler, and A Li. Automatic, Intelligent Commercial SSA Sensor Scheduling, AMOS Conference, Maui, HI, 2019.

[2] N, Estell, D Ma, and P Seitzer, Daylight Imaging of LEO Satellites Using COTS Hardware, AMOS Conference, Maui, HI, 2019.